Observed Increase of TTL Temperature and Water Vapor in Polluted Clouds over Asia

HUI SU,* JONATHAN H. JIANG,* XIAOHONG LIU,+ JOYCE E. PENNER,# WILLIAM G. READ,* STEVEN MASSIE,@ MARK R. SCHOEBERL,&,**,++ PETER COLARCO,& NATHANIEL J. LIVESEY,* AND MICHELLE L. SANTEE*

* *Jet Propulsion Laboratory, California Institute of Technology, Pasadena, California*
+ *Pacific Northwest National Laboratory, Richland, Washington*
# *Department of Atmospheric, Oceanic, and Space Sciences, University of Michigan, Ann Arbor, Michigan*
@ *National Center for Atmospheric Research, Boulder, Colorado*
& *NASA Goddard Space Flight Center, Greenbelt, Maryland*

(Manuscript received 23 March 2010, in final form 13 December 2010)

ABSTRACT

Satellite observations are analyzed to examine the correlations between aerosols and the tropical tropopause layer (TTL) temperature and water vapor. This study focuses on two regions, both of which are important pathways for the mass transport from the troposphere to the stratosphere and over which Asian pollution prevails: South and East Asia during boreal summer and the Maritime Continent during boreal winter. Using the upper-tropospheric carbon monoxide measurements from the *Aura* Microwave Limb Sounder as a proxy of aerosols to classify ice clouds as polluted or clean, the authors find that polluted clouds have a smaller ice effective radius and a higher temperature and specific humidity near the tropopause than clean clouds. The increase in water vapor appears to be related to the increase in temperature, as a result of increased aerosols. Meteorological differences between the clouds cannot explain the differences in temperature and water vapor for the polluted and clean clouds. The authors hypothesize that aerosol semidirect radiative heating and/or changes in cirrus radiative heating, resulting from aerosol microphysical effects on clouds, may contribute to the increased TTL temperature and thus increased water vapor in the polluted clouds.

1. Introduction

Water vapor is a strong greenhouse gas that acts to amplify surface warming caused by anthropogenic greenhouse gases (e.g., CO_2). In the stratosphere, water vapor also plays a major role in ozone chemistry and serves as a reliable dynamical tracer because of its long lifetime. The mechanisms that control the amount of stratospheric water vapor are not fully understood (e.g., Solomon et al. 2010). The current understanding is that the entry value of water vapor mixing ratio into the stratosphere is largely determined by the cold-point tropopause temperature (CPT), through which air is freeze dried during slow ascent from the troposphere to the stratosphere (Holton and Gettelman 2001; Fueglistaler et al. 2005; Randel et al. 2006; Read et al. 2004). Several other processes may modify stratospheric water vapor abundance. For example, overshooting convection detrains cold and dry air, which dehydrates the stratosphere, while evaporation of detrained small ice crystals may rehydrate the tropical tropopause layer (TTL) (Sherwood and Dessler 2001; Dessler 2002; Jensen et al. 2007). The radiative heating from subvisible cirrus clouds near the tropopause can act to increase stratospheric water vapor by increasing tropopause temperature (Rosenfield et al. 1998). A linkage between aerosols and transport of water vapor to the stratosphere was proposed by Sherwood (2002a). He postulated that aerosols from biomass burning may reduce ice cloud effective radius R_e near the top of cumulus towers, leading to a decrease in the settling velocity of ice crystals, an increase in ice sublimation, and hence increased stratospheric water vapor. A modeling

** Retired.
++ Current affiliation: Science and Technology Corporation, Lanham, Maryland.

Corresponding author address: Hui Su, Jet Propulsion Laboratory, California Institute of Technology, Pasadena, CA 91109.
E-mail: hui.su@jpl.nasa.gov

DOI: 10.1175/2010JCLI3749.1

© 2011 American Meteorological Society

study by Notholt et al. (2005) showed that increasing anthropogenic SO_2 emissions in Asia may increase the formation of sulfuric acid aerosols and thus small ice crystals in the TTL, which are lifted into the stratosphere and increase stratospheric humidity when they evaporate. More recently, Liu et al. (2009) showed that increasing anthropogenic sulfate and soot concentrations in a global aerosol–climate model lead to increased ice clouds and water vapor in the upper troposphere (UT) and lower stratosphere (LS). In Liu et al. (2009), homogeneous ice nucleation on sulfate, heteorogeneous ice nucleation on soot, and the competition between the two nucleation mechanisms were considered (Liu and Penner 2005). These earlier studies suggested that aerosols may affect stratospheric water vapor through their interactions with ice clouds. In addition, Lau and Kim (2006) and Lau et al. (2006) indicate that direct radiative heating of absorbing aerosols such as dust and black carbon (BC) may cause UT warming and moistening over the Tibetan Plateau during the Asian monsoon season. Panels 4b and 4c in Lau et al. (2006) display model temperature anomalies of 1 and 2.5 K over the Himalayas in April and May, respectively, due to the effects of absorbing aerosols, although Kuhlmann and Quaas (2010) obtained smaller heating rates over the Tibetan Plateau by analyzing Cloud–Aerosol Lidar and Infrared Pathfinder Satellite Observations (CALIPSO) aerosol data during March–May 2007, 2008, and 2009. However, observational evidence of aerosol influence on stratospheric water vapor has been lacking.

The ''A-Train'' constellation of satellites provides a suite of measurements that can shed light on the interplay among aerosols, clouds, and water vapor (L'Ecuyer and Jiang 2010). In particular, the Microwave Limb Sounder (MLS) on *Aura* satellite measures global profiles of water vapor (H_2O), temperature T, ice water content (IWC), and carbon monoxide (CO) in the UTLS, and the *Aqua* Moderate-Resolution Imaging Spectroradiometer (MODIS) provides aerosol optical thickness (AOT) and ice cloud particle size in terms of R_e. Jiang et al. (2008, 2009) showed that MLS in-cloud CO at 215 hPa bears a close correlation to aerosol loading in many convective regions and can, in these regions, be used as an index for aerosol amount. In addition, a recent study using measurements from 11 airborne campaigns in the Pacific hemisphere (Clarke and Kapustin 2010) confirmed that increasing aerosols is associated with enhanced CO in the Asian region. Combining MLS CO and IWC with MODIS AOT and R_e and Tropical Rainfall Measuring Mission (TRMM) precipitation, Jiang et al. (2008, 2009) found that polluted clouds are associated with smaller ice particle size and weaker precipitation than clean clouds in a number of regions and seasons. With these observations, we explore here the correlations of pollution aerosols (indicated by CO) with temperature and water vapor in the TTL region, a critical layer for water vapor transport from the troposphere to the stratosphere. Identification of the observed relationship is the first step to establishing the linkage between aerosols and stratospheric water vapor and to understanding the physical mechanisms. We also attempt to separate the role of dynamics from aerosol effects by contrasting the temperature and water vapor changes associated with changes in meteorological conditions to those associated with aerosol changes. For dynamical variables, we use the *Aqua* Atmospheric Infrared Sounder (AIRS) temperature and water vapor profiles and the derived convective available potential energy (CAPE), as well as the midtropospheric vertical pressure velocity at 500 hPa ω_{500} and divergence from the National Centers for Environmental Prediction (NCEP).

The structure of the paper is as follows. Section 2 describes the observational datasets and our analysis approach. Section 3 presents the data analysis results. Discussion and conclusions are given in section 4.

2. Datasets and analysis approach

In this study, we primarily use *Aura* MLS observations (V2.2) of H_2O, T, IWC, and CO, and *Aqua* MODIS AOT (MYD04-L2) and R_e (MYD08-D3) data from 2005 to 2008. The MLS data have a horizontal resolution of ~300 km along track and ~7 km cross track. The vertical resolutions for H_2O (and T), IWC, and CO are about 3, 4, and 5 km, respectively. We are interested in the H_2O and T measurements in the TTL, a transition zone between the UT and LS. The estimated MLS measurement accuracies are within 20% for H_2O, a factor of 2 for IWC and about 0.5–1 K for T at 147 and 100 hPa (Read et al. 2007; Wu et al. 2008; Schwartz et al. 2008). The IWC detection thresholds are 0.6 mg m^{-3} at 215 hPa, 0.1 mg m^{-3} at 147 hPa, and 0.02 mg m^{-3} at 100 hPa (Wu et al. 2008). The MLS H_2O, T, and IWC are independent products from radiances in different MLS channels. The uncertainty in the temperature retrieval minimally affects the H_2O retrieval (~2%) (Read et al. 2007). The MLS measurements at these altitudes are generally not degraded by the presence of clouds and aerosols, whose particle sizes are typically much smaller than the measurement wavelengths. Very thick clouds (IWC > ~50 mg m^{-3}) can degrade the temperature and some species measurements (Wu et al. 2008), but the retrieval algorithms (Livesey et al. 2006) flag such measurements and they are not used here. The V2.2 CO at 215 hPa has a factor of 2 high bias, but the morphology is validated to be reasonable (Livesey et al. 2008).

The MODIS ice cloud R_e measurement refers to the top of cirrus clouds, with the vertical averaging kernel peaked at about 0.1–0.2 optical depth ($<\sim$1–2 km depending on cloud extinction) down from the cloud top (Platnick 2000; Zhang et al. 2010). We use MODIS R_e measurements that are collocated with detectable MLS IWC. The low biases in the R_e retrieval do not affect our results as we are interested in the relative differences in R_e between polluted and clean clouds. The MODIS AOT is a columnar quantity with a horizontal resolution of 10 km $\times$ 10 km. Although it is likely that aerosols are mostly distributed in the boundary layer, they can influence ice clouds by acting as cloud condensation nuclei (CCN) and altering liquid cloud particle sizes, which are subsequently lifted by deep convection to form ice clouds (Sherwood 2002b). Thus, using AOT to represent aerosol loadings is acceptable. We average the MODIS data onto 3° $\times$ 1° boxes centered on the MLS measurement locations to obtain collocated MODIS and MLS measurements.

We derive the CAPE using the *Aqua* AIRS Level 3 temperature and water vapor measurements, assuming air parcels rising from the surface along pseudoadiabats. The AIRS data at the original 1° $\times$ 1° resolution are resampled on the MLS footprints. Similar resampling for the NCEP reanalysis data is performed.

Following Jiang et al. (2008), we use MLS CO at 215 hPa as a proxy for aerosols to classify ice clouds as ''polluted'' or ''clean.'' As in-cloud aerosols cannot be measured by satellites, using CO gives us about 3–4 times the number of samples of collocated pollution, clouds, and H_2O than obtained by simply using AOT in adjacent cloud-free regions, ensuring a higher signal-to-noise ratio and greater statistical significance. Compared to the CO at 147 and 100 hPa, the 215-hPa CO has the strongest correlation with surface emission coincident with convection (Jiang et al. 2007). For this study, we define clean ice clouds to be the instantaneous measurements that have detectable MLS IWC throughout 215–100 hPa and MLS CO at 215 hPa less than 100 ppbv. The choice of the CO threshold value is made considering that the background CO value at 215 hPa is about 40–60 ppbv and the MLS V2.2 215 hPa CO measurement has a factor of $\sim$2 high bias (Livesey et al. 2008). Polluted ice clouds are those meeting the same IWC criterion but with 215-hPa CO greater than 240 ppbv in June–August (JJA) and 200 ppbv in December–February (DJF). By definition, these clouds, both clean and polluted, are mostly deep convective clouds and associated anvils. The average fraction of polluted clouds out of the total valid measurement ensemble is 3.2% in JJA over South and East Asia (SEA, 685 profiles) and 1.8% in DJF Maritime Continent (MTC, 449 profiles), and the fraction of clean clouds is close to 1% in both cases (157 profiles in JJA SEA and 236 profiles in DJF MTC). Our definitions of polluted and clean clouds represent the two extreme ends (the lowest and highest 1%–3%) of the cloud spectrum, so that a distinct signal of aerosol effects can be extracted. Using lower (higher) threshold values of CO to define polluted (clean) clouds produces qualitatively similar results, but with weaker statistical significance. Clouds that are not ''deep'' or have intermediate CO values are not considered.

As the cloud properties (R_e, H_2O, and T) of interest are strongly correlated with convective intensity, we compare the polluted and clean cloud properties binned as a function of MLS 215-hPa IWC, which correlates well with outgoing longwave radiation and serves as a measure of convective strength (Su et al. 2006; Jiang et al. 2011). This binning on IWC also helps to decouple the UT CO changes due to changes in surface CO emission and convective strength. For deep clouds with the same IWC, the UT CO difference can be mostly attributed to differences in surface emission (related to AOT) rather than differences in convective strength.

Moreover, examining the cloud properties binned as a function of 215-hPa IWC is equivalent to holding convective influences constant to isolate aerosols or other nonconvective effects. This is particularly important as multiple nonindependent factors (e.g., convection and aerosols) may act together to determine the TTL temperature and water vapor. For example, deep convection can change the temperature and aerosol loading in the air column, while aerosol effects may alter convective strength and atmospheric temperature. To isolate the aerosol effects on the TTL temperature and water vapor, it is important to hold dynamic and thermodynamic conditions constant when examining the differences in temperature and water vapor for different aerosol loadings. This can be approximately achieved by binning observational samples according to pollution and meteorological conditions simultaneously. By alternating the binning variables, we search for statistically significant signals emerging from combinations of sample properties that provide a meaningful indication of physical processes. The binning approach automatically averages out random noise. Since the differences between two groups of samples are of interest, the biases in the observational data have little impact on the interpretation of the results.

3. Observational analysis of Asian polluted regions

We choose two analysis regions, both of which are important pathways for water vapor transport to the stratosphere and experience heavy pollution from Asian countries with rapidly growing economies. One area is

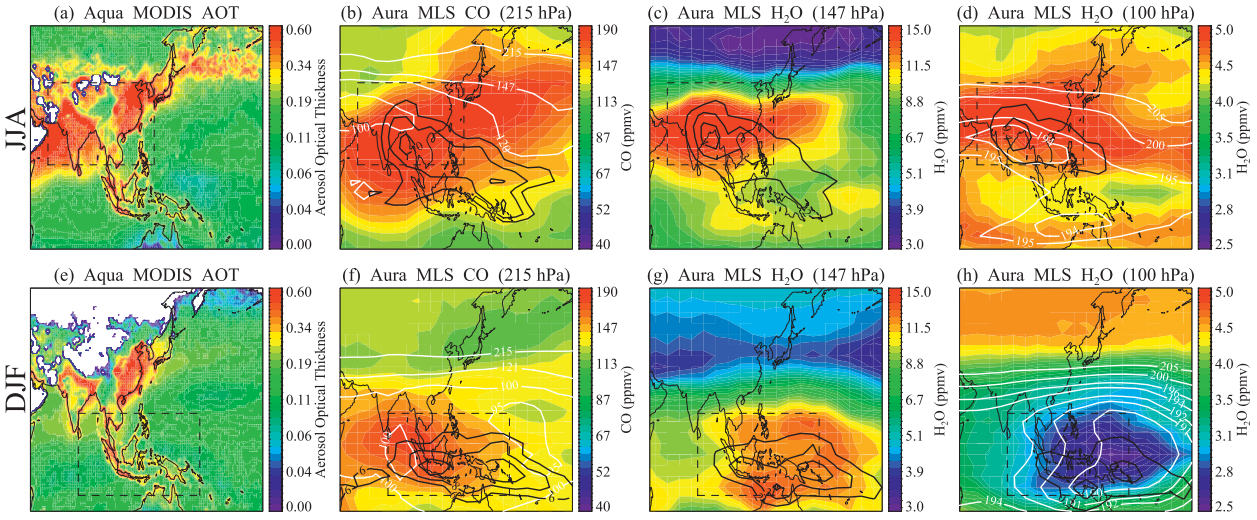

FIG. 1. Maps of AOT, UT CO, H_2O, and IWC averaged for 2005–08, with (a)–(d) JJA and (e)–(h) DJF. (a),(e) MODIS AOT; (b),(f) MLS 215-hPa CO (shaded) and IWC (black contours at 2 mg m^{-3} interval), with white contours indicating the *GEOS-5* lapse-rate tropopause pressure; (c),(g) MLS 147-hPa H_2O (shaded) and IWC (black contours at 1 mg m^{-3} interval); and (d),(h) MLS 100-hPa H_2O (shaded) and IWC (black contours at 0.2 mg m^{-3} interval), with white contours indicating MLS temperature at 100 hPa. The analysis region in each season is marked by the dashed box.

SEA (10°–40°N, 60°–130°E) in JJA. Prior studies have shown that the Asian summer monsoon circulation over this region provides an important pathway for water vapor and pollution transport into the global stratosphere (Fu et al. 2006; Randel et al. 2010). The other analysis region is the MTC (15°S–15°N, 80°–160°E) in DJF. During boreal winter, the MTC region is very cold and extremely important in determining the entry value of water vapor mixing ratio into the stratosphere (the so-called stratospheric fountain, Newell and Gould-Stewart 1981). It is also a region into which Asian pollution is preferentially transported (Stohl et al. 2002).

Figure 1 shows maps of 2005–08 JJA and DJF average MODIS AOT, MLS CO, and IWC at 215 hPa, and MLS water vapor and IWC at 147 and 100 hPa, encompassing the two analysis regions (dashed boxes). The 147 and 100 hPa pressure levels approximately correspond to the bottom of the TTL and the height of the CPT, respectively. During boreal summer, the spatial distribution of 215-hPa CO resembles that of AOT; although enhanced CO is more widespread than high AOT, consistent with the expectation that CO, unlike aerosols, is not subject to wet removal by clouds and precipitation and thus is of longer lifetime than aerosols. The SEA region has the highest AOT and CO, coincident with high H_2O and IWC at 147 and 100 hPa. The anticyclone over the Tibetan Plateau traps high CO and H_2O, providing a significant source of trace gases to the stratosphere (Li et al. 2005; Fu et al. 2006; Park et al. 2009; Randel et al. 2010). During boreal winter, Figs. 1e and 1f show that the MLS CO at 215 hPa is quite high over the entire MTC region, while high AOT is concentrated over land (islands) and is relatively low over ocean. The high CO may include pollution advected from South and East Asia at lower levels that is uplifted to the UT by deep convection (indicated by the IWC contours at 215 hPa, also see Fig. 2 in Stohl et al. 2002). Water vapor is relatively high over the MTC at 147 hPa because of strong convection, but it reaches a minimum at 100 hPa associated with the low temperature. Based on the Goddard Earth Observing System Model (version 5) analyses, the average thermal tropopause height (Figs. 1b and 1f) over DJF MTC is around 90–100 hPa, higher than the 100–120 hPa seen in JJA SEA.

Figure 2 shows that polluted clouds defined by CO are associated with higher AOT than clean clouds for most values of IWC in both regions, except at large IWCs where aerosols are likely to be removed by precipitation. The aerosol concentrations are significantly higher in SEA than in MTC. The averaged difference in AOT for all IWCs between polluted and clean clouds is about 0.21 (~45%) in SEA and 0.04 (~16%) in MTC. For a given IWC, these polluted convective clouds have a smaller R_e than clean clouds, as noted previously (Jiang et al. 2008, 2009; Sherwood 2002a). The average R_e difference is about 1–2 μm (5%–10%). For ice clouds formed in situ, a few previous studies have indicated that increasing aerosols may not necessarily lead to reduced ice cloud particle size (e.g., DeMott et al. 2003 and references 5–7 therein). In JJA SEA, polluted clouds have higher H_2O and temperature than clean clouds at both 147 and 100 hPa; these differences extend up to 83 hPa. In DJF

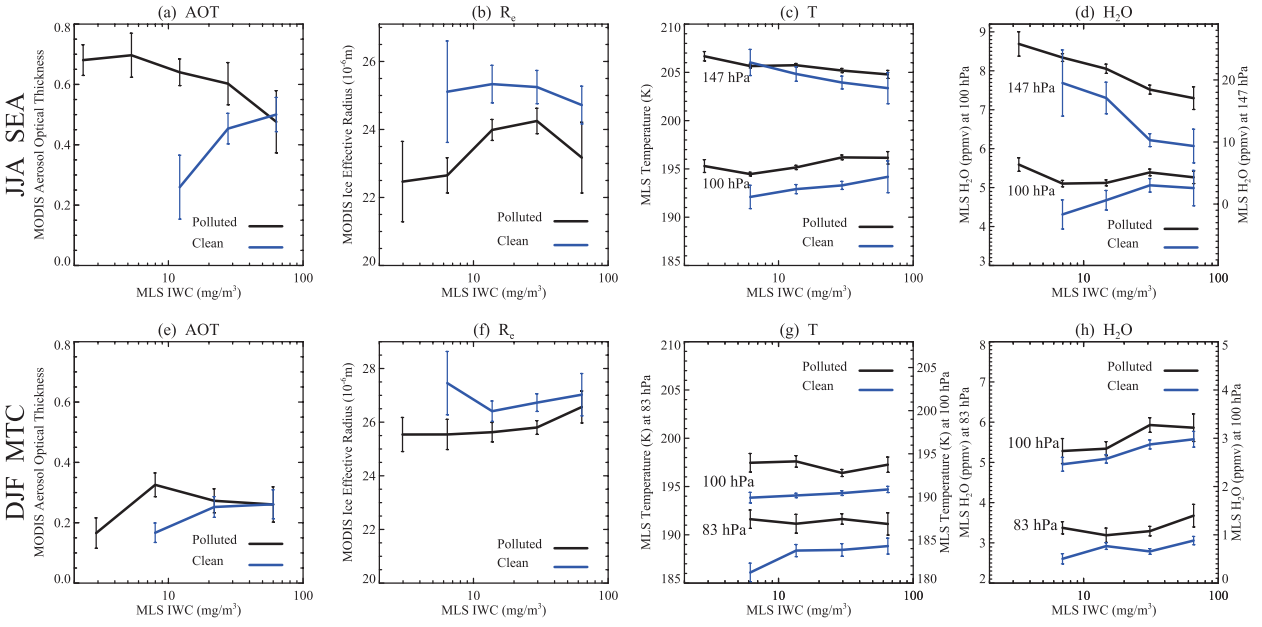

FIG. 2. AOT, ice cloud particle size, temperature, and TTL H_2O for polluted and clean clouds, binned as a function of 215-hPa MLS IWC, with (a)–(d) JJA SEA and (e)–(h) DJF MTC. (a),(e) MODIS AOT; (b),(f) MODIS ice cloud effective radius R_e; (c),(g) MLS temperature; and (d),(h) MLS H_2O. The error bars denote the standard errors ($\sigma/\sqrt{N}$) of the bin averages.

MTC, the increased H_2O and temperature in polluted clouds are evident at 121, 100, and 83 hPa but insignificant at 147 hPa, probably because of the higher tropopause and convective detrainment height in this region than in JJA SEA. In both cases, the H_2O difference at 100 hPa is approximately 0.2–0.5 ppmv, and the temperature difference is about 2 K. These differences are comparable to the magnitudes of the interannual anomalies for 100-hPa H_2O and temperature driven by large-scale dynamics (Fueglistaler and Haynes 2005). At 100 hPa, polluted clouds have lower relative humidity with respect to ice (RHi) than clean clouds, as the change in temperature dominates over the change in H_2O (figure not shown). The statistical significance of the different means between the polluted and clean clouds is examined using the two-sided Student's t test for all IWC bins (see the appendix). We find that the mean properties (AOT, R_e, T, and H_2O) for the polluted and clean clouds in each IWC bin are statistically different with 95% or greater confidence. When the error bars are large and nearly overlapping, the statistical significance is, as expected, low. Most of the differences shown in Fig. 2 are statistically significant at 95% confidence.

In Fig. 2, the 215-hPa IWC serves as an index for convective strength. The binning of cloud properties as a function of 215-hPa IWC is important in two aspects. First, given the same convective strength, the different UT CO amounts in the polluted and clean clouds can be mostly attributed to differences in underlying pollution amount, as shown by AOT in Figs. 2a and 2e. Second, the influence of convective strength is held approximately constant when we compare the differences in R_e, H_2O, and T between polluted and clean cases binned in the same IWC intervals. Hence, the differences we observe are more likely contributed by aerosol effects, rather than by differences in dynamics. We have also used the NCEP ω_{500} or 200-hPa divergence as alternative indices for convective strength. The results (not shown) are similar to those obtained from binning by the 215-hPa IWC.

One may conjecture that the increases of water vapor are caused by increases of temperature. To investigate this, we bin the polluted and clean cloud samples by their 100-hPa temperature rather than by their IWC at 215 hPa (Fig. 3). When 100-hPa T is held constant, the differences in 100-hPa H_2O for the polluted and clean clouds nearly vanish over the temperature range that they overlap (except at T around 200 K in JJA SEA), confirming the dominance of 100-hPa temperature in controlling the 100-hPa water vapor. There is also an indication that the polluted clouds generally have higher mean 100-hPa temperature than the clean clouds during boreal summer in SEA.

To test whether the 100-hPa T and H_2O differences in the polluted and clean clouds may simply arise from different meteorological conditions, we group these cloud samples by their meteorological conditions instead of by their pollution loadings. Figure 4 shows that there is no significant difference in 100 hPa T and H_2O between the

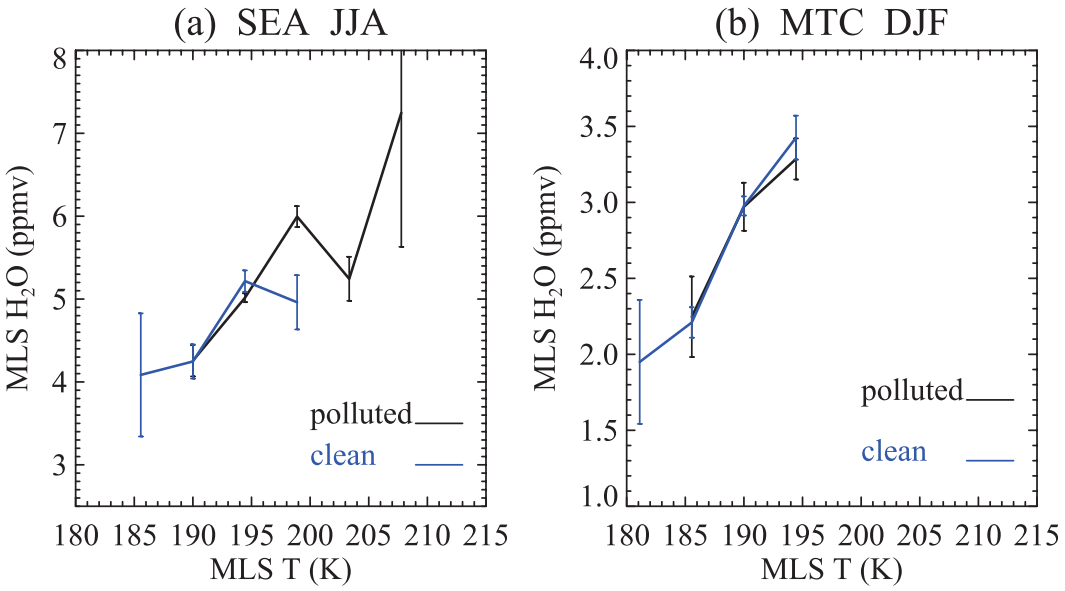

FIG. 3. The 100-hPa H_2O for the polluted and clean clouds binned as a function of 100-hPa temperature for (a) JJA SEA and (b) DJF MTC.

two groups of samples separated by different lower-tropospheric (850 hPa) humidity or CAPE from AIRS, nor by 850-hPa convergence or ω_{500} from NCEP, as indicated by the overlapping error bars. Grouping by ω_{500} or CAPE shows some separation in 100-hPa T and H_2O in some IWC bins, but the results are not consistent across all IWC bins. Similar results are found for 83- and 121-hPa H_2O and for all deep clouds with intermediate CO values. The overlapping error bars are not sensitive to the cutoff values of the meteorological parameters chosen for grouping; taking a certain percentile of the samples results in even larger error bars, making a separation

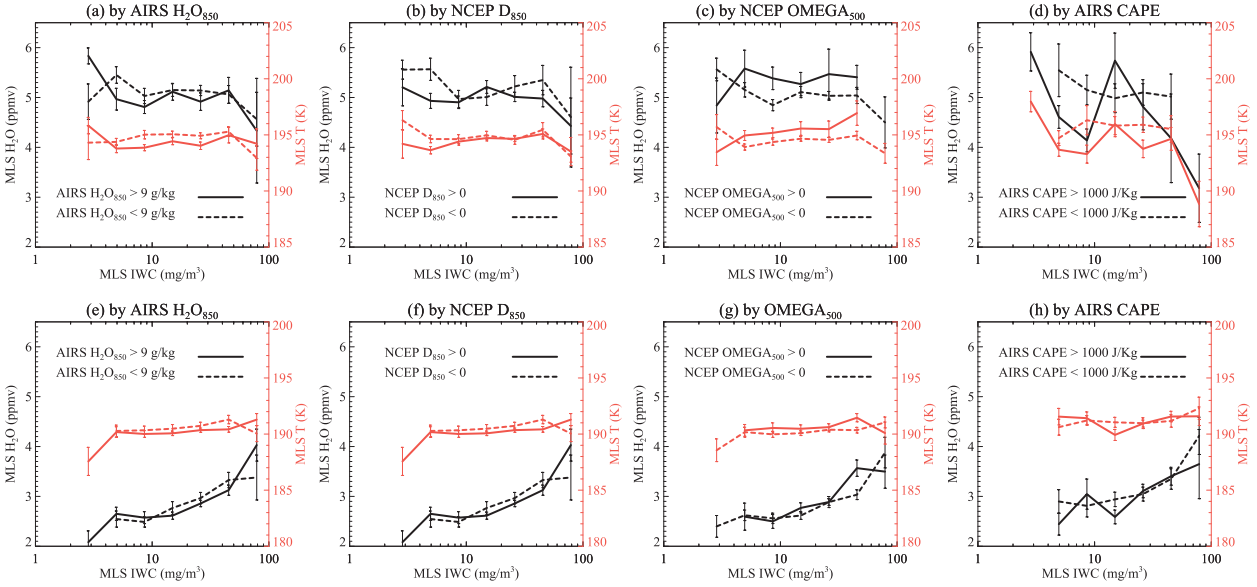

FIG. 4. 100-hPa H_2O (black) and T (red) grouped by their meteorological conditions: (a) by AIRS 850-hPa water vapor mixing ratio; (b) by NCEP divergence at 850 hPa; (c) by NCEP ω_{500}; and (d) by CAPE calculated from AIRS temperature and water vapor soundings. The choice of threshold values for each grouping ensures approximately the same number of samples for each group. All properties are binned as a function of 215-hPa MLS IWC, with (a)–(d) JJA SEA and (e)–(h) DJF MTC. The error bars denote the standard errors ($\sigma/\sqrt{N}$) of the bin averages.

TABLE A1. The probability (%) of the polluted and clean clouds having different means for several IWC bins using the Student's *t* test with unequal variance samples. The top row indicates the center values of IWC for the bins of the standard errors shown in Fig. 2 of the manuscript.

	IWC 5.4 mg m^{-3}		IWC 12.4 mg m^{-3}		IWC 28.3 mg m^{-3}		IWC 64.7 mg m^{-3}	
	JJA SEA	DJF MTC	JJA SEA	DJF MTC	JJA SEA	DJF MTC	JJA SEA	DJF MTC
AOT	N/A	99.25	87.06	30.25	90.86	N/A	15.74	0.65
R_e	80.15	84.32	95.96	86.13	88.99	97.29	80.22	35.58
T (147 and 100 hPa in SEA;	20.19	99.66	74.32	99.64	91.72	100.0	58.31	99.18
100 and 83 hPa in MTC)	100.0	99.96	99.98	97.69	100.0	99.96	70.69	87.95
H_2O (147 and 100 hPa in SEA;	53.06	63.66	91.08	77.45	100.0	97.28	96.40	52.4
100 and 83 hPa in MTC)	87.81	99.69	99.98	73.54	100.0	99.65	70.69	89.35

between groups more indiscernible. Only when these clouds are grouped by their pollution loadings, as shown in Fig. 2, is a clear separation in 100-hPa *T* and H_2O attained.

4. Discussion and conclusions

Analyzing the collocated temperature, water vapor, clouds, and pollution (CO and AOT) data, we have presented an observed linkage of pollution aerosols with the TTL temperature and water vapor, which is relevant to the water vapor transport from the troposphere to the stratosphere. The aerosol-induced water vapor change at 100 hPa in heavily polluted cloudy regions is up to 0.5 ppmv, comparable in magnitude to the interannual variations of stratospheric water vapor. The change of water vapor is associated with temperature changes near the tropopause. Differences in meteorological conditions (Fig. 4) do not correspond to as statistically significant differences in temperature and water vapor as do different pollution loadings (Fig. 2). Since our analyses are focused on two specific regions and seasons, the seasonal cycle and large-scale dynamic influence on temperature variations are minimized. The factor remaining that can be responsible for the temperature difference between polluted and clean clouds appears to be the pollution amount.

As our analysis pertains to deep ice clouds, we hypothesize that both direct and indirect effects of aerosols may be responsible for the increased TTL temperature. On the one hand, aerosols can be uplifted to the upper troposphere by deep convection. Since Asian pollution consists of large amounts of absorbing aerosols such as black carbon, the semidirect effect of absorbing aerosols may cause a local heating in the TTL. This is in line with the "Elevated-Heat-Pump" (EHP) effect proposed by Lau and Kim (2006) and Lau et al. (2006). On the other hand, the reduction of cirrus cloud particle size associated with increasing aerosols suggests that aerosols also alter the cirrus cloud properties (Figs. 2b and 2f). This can be achieved by aerosol microphysical effects on liquid clouds, which are subsequently lifted to form ice clouds of small particle sizes. In this case, even if aerosols are concentrated in the boundary layer, they can exert an impact on the cirrus clouds through deep convection (Sherwood 2002a). Smaller ice particles can produce greater local radiative heating than larger ice particles with the same IWC (Fu and Liou 1993). They also fall more slowly and have longer residence time, which may also contribute to a stronger heating effect in the TTL. However, the exact mechanisms cannot be determined from current observations alone.

The aerosol correlations with the TTL water vapor we emphasize here are complementary to the microphysical linkage among aerosols, cumulus, and stratospheric water vapor proposed in Sherwood (2002a). In Sherwood (2002a), the smaller ice particles caused by aerosol indirect effects evaporate more efficiently in a subsaturated environment, thus moistening the UT/LS. This mechanism is not necessarily accompanied by significant changes in the TTL temperature, while in our observational correlations, the change of TTL temperature is necessary for the change of TTL water vapor.

As discussed in the introduction, higher TTL temperature and water vapor may lead to increased water vapor transport into the stratosphere. Although the heavily polluted deep clouds, as we have defined them, account for only 1%–3% of the total collocated cloud and CO measurements, it may be important for climate models to take into account the aerosol moistening mechanism to accurately predict climate change. Further studies are needed to determine how changes in Asian pollution, superimposed on natural variability, perturb global stratospheric water vapor variations.

Acknowledgments. We thank the funding support from the NASA ACMAP, AST, and IDS programs. XL and JEP acknowledge the support from the DOE Atmospheric System Research Program. The Pacific Northwest National Laboratory is operated for the DOE by Battelle Memorial Institute under Contract DE-AC06-76RLO 1830. Discussions with Daniel Rosenfeld are greatly appreciated. This work was performed at the Jet Propulsion Laboratory, California Institute of Technology, under

contract with NASA. NCAR is supported by the National Science foundation.

APPENDIX

Statistical Test of the Results

The two-sided Student's *t* test with unequal variance is used to examine the statistical significance of the two sample means for the polluted and clean clouds shown in Fig. 2. Table A1 shows the statistical significance for the different means in each IWC bins where the standard error bars ($\sigma/\sqrt{N}$) are marked. In general, the smaller errors and the larger distance between the polluted and clean error bars, the higher significance of the different means.

REFERENCES

Clarke, A., and V. Kapustin, 2010: Hemispheric aerosol vertical profiles: Anthropogenic impacts on optical depth and cloud nuclei. *Science,* **329,** 1488.

DeMott, P. J., D. J. Cziczo, A. J. Prenni, D. M. Murphy, S. M. Kreidenweis, D. S. Thompson, R. Porys, and D. C. Rogers, 2003: Measurements of the concentration and composition of nuclei for cirrus formation. *Proc. Natl. Acad. Sci. USA,* **100,** 14 655–14 660.

Dessler, A. E., 2002: The effect of deep, tropical convection on the tropical tropopause layer. *J. Geophys. Res.,* **107,** 4033, doi:10.1029/2001JD000511.

Fu, Q., and K. N. Liou, 1993: Parameterization of the radiative properties of cirrus clouds. *J. Atmos. Sci.,* **50,** 2008–2025.

Fu, R., and Coauthors, 2006: Short circuit of water vapor and polluted air to the global stratosphere by convective transport over the Tibetan Plateau. *Proc. Natl. Acad. Sci. USA,* **103,** 5664–5669.

Fueglistaler, S., and P. H. Haynes, 2005: Control of interannual and longer-term variability of stratospheric water vapor. *J. Geophys. Res.,* **110,** D24108, doi:10.1029/2005JD006019.

——, M. Bonazzola, P. H. Haynes, and T. Peter, 2005: Stratospheric water vapor predicted from the Lagrangian temperature history of air entering the stratosphere in the tropics. *J. Geophys. Res.,* **110,** D08107, doi:10.1029/2004JD005516.

Holton, J. R., and A. Gettelman, 2001: Horizontal transport and the dehydration of the stratosphere. *Geophys. Res. Lett.,* **28,** 2799–2802.

Jensen, E. J., A. S. Ackerman, and J. A. Smith, 2007: Can overshooting convection dehydrate the tropical tropopause layer? *J. Geophys. Res.,* **112,** D11209, doi:10.1029/2006JD007943.

Jiang, J. H., N. J. Livesey, H. Su, L. Neary, J. C. McConnell, and N. A. Richards, 2007: Connecting surface emissions, convective uplifting, and long-range transport of carbon monoxide in the upper troposphere: New observations from the Aura Microwave Limb Sounder. *Geophys. Res. Lett.,* **34,** L18812, doi:10.1029/2007GL030638.

——, H. Su, M. Schoeberl, S. T. Massie, P. Colarco, S. Platnick, and N. Livesey, 2008: Clean and polluted clouds: relationships among pollution, ice cloud and precipitation in South America. *Geophys. Res. Lett.,* **35,** L14804, doi:10.1029/2008GL034631.

——, ——, S. T. Massie, P. Colarco, M. Schoeberl, and S. Platnick, 2009: Aerosol-CO relationship and aerosol effect on ice cloud particle size: Analyses from Aura MLS and Aqua MODIS observations. *J. Geophys. Res.,* **114,** D20207, doi:10.1029/2009JD012421.

——, and Coauthors, 2011: Influence of convection and aerosol pollution on ice cloud particle effective radius. *Atmos. Chem. Phys.,* **11,** 457–463, doi:10.5194/acp-11-457-2011.

Kuhlmann, J., and J. Quaas, 2010: How can aerosols affect the Asian summer monsoon? Assessment during three consecutive pre-monsoon seasons from CALIPSO satellite data. *Atmos. Chem. Phys.,* **10,** 4673–4688.

Lau, K. M., and K. M. Kim, 2006: Observational relationships between aerosol and Asian monsoon rainfall, and circulation. *Geophys. Res. Lett.,* **33,** L21810, doi:10.1029/2006GL027546.

——, M. K. Kim, and K. M. Kim, 2006: Asian summer monsoon anomalies induced by aerosol direct forcing: The role of the Tibetan Plateau. *Climate Dyn.,* **26,** 855–864.

L'Ecuyer, T. S., and J. H. Jiang, 2010: Touring the atmosphere aboard the A-Train. *Phys. Today,* **63,** 36–41.

Li, Q. B., and Coauthors, 2005: Convective outflow of South Asian pollution: A global CTM simulation compared with EOS MLS observations. *Geophys. Res. Lett.,* **32,** L14826, doi:10.1029/2005GL022762.

Liu, X., and J. E. Penner, 2005: Ice nucleation parameterization for global models. *Meteor. Z.,* **14,** 499–514.

——, ——, and M. Wang, 2009: Influence of anthropogenic sulfate and black carbon on upper tropospheric clouds in the NCAR CAM3 model coupled to the IMPACT global aerosol model. *J. Geophys. Res.,* **114,** D03204, doi:10.1029/2008JD010492.

Livesey, N. J., W. V. Snyder, W. G. Read, and P. A. Wagner, 2006: Retrieval algorithms for the EOS Microwave Limb Sounder (MLS) instrument. *IEEE Trans. Geosci. Remote Sens.,* **44,** 1144–1155.

——, and Coauthors, 2008: Validation of Aura Microwave Limb Sounder O_3 and CO observations in the upper troposphere and lower stratosphere. *J. Geophys. Res.,* **113,** D15S02, doi:10.1029/2007JD008805.

Newell, R. E., and S. Gould-Stewart, 1981: A stratospheric fountain? *J. Atmos. Sci.,* **38,** 2789–2796.

Notholt, J., and Coauthors, 2005: Influence of tropospheric SO_2 emissions on particle formation and the stratospheric humidity. *Geophys. Res. Lett.,* **32,** L07810, doi:10.1029/2004GL022159.

Park, M., W. J. Randel, L. K. Emmons, and N. J. Livesey, 2009: Transport pathways of carbon monoxide in the Asian summer monsoon diagnosed from Model of Ozone and Related Tracers (MOZART). *J. Geophys. Res.,* **114,** D08303, doi:10.1029/2008JD010621.

Platnick, S., 2000: Vertical photon transport in cloud remote sensing problems. *J. Geophys. Res.,* **105,** 22 919–22 935.

Randel, W. J., F. Wu, H. Vomel, G. E. Nedoluha, and P. Forster, 2006: Decreases in stratospheric water vapor after 2001: Links to changes in the tropical tropopause and the Brewer–Dobson circulation. *J. Geophys. Res.,* **111,** D12312, doi:10.1029/2005JD006744.

——, M. Park, L. Emmons, D. Kinnison, P. Bernath, K. A. Walker, C. Boone, and H. Pumphrey, 2010: Asian monsoon transport of pollution to the stratosphere. *Science,* **328,** 611–613.

Read, W. G., D. L. Wu, J. W. Waters, and H. C. Pumphrey, 2004: Dehydration in the tropical tropopause layer: Implications from UARS MLS. *J. Geophys. Res.,* **109,** D06110, doi:10.1029/2003JD004056.

——, and Coauthors, 2007: Aura Microwave Limb Sounder upper tropospheric and lower stratospheric H_2O and relative

humidity with respect to ice validation. *J. Geophys. Res.,* **112,** D24S35, doi:10.1029/2007JD008752.

Rosenfield, J., D. Considine, M. Schoeberl, and E. Browell, 1998: The impact of subvisible cirrus clouds near the tropical tropopause on stratospheric water vapor. *Geophys. Res. Lett.,* **25,** 1883–1886.

Schwartz, M. J., and Coauthors, 2008: Validation of the Aura Microwave Limb Sounder temperature and geopotential height measurements. *J. Geophys. Res.,* **113,** D15S11, doi:10.1029/2007JD008783.

Sherwood, S. C., 2002a: A microphysical connection among biomass burning, cumulus clouds, and stratospheric moisture. *Science,* **295,** 1272–1275.

——, 2002b: Aerosols and ice particle size in tropical cumulonimbus. *J. Climate,* **15,** 1051–1063.

——, and A. E. Dessler, 2001: A model for transport across the tropical tropopause. *J. Atmos. Sci.,* **58,** 765–779.

Solomon, S., K. Rosenlof, R. Portmann, J. Daniel, S. Davis, T. Sanford, and G. Plattner, 2010: Contributions of stratospheric water vapor to decadal changes in the rate of global warming. *Science,* **303,** 1219–1223.

Stohl, A., S. Eckhardt, C. Forster, P. James, and N. Spichtinger, 2002: On the pathways and timescales of intercontinental air pollution transport. *J. Geophys. Res.,* **107,** 4684, doi:10.1029/2001JD001396.

Su, H., W. G. Read, J. H. Jiang, J. W. Waters, D. L. Wu, and E. J. Fetzer, 2006: Enhanced positive water vapor feedback associated with tropical deep convection: New evidence from Aura MLS. *Geophys. Res. Lett.,* **33,** L05709, doi:10.1029/2005GL025505.

Wu, D. L., and Coauthors, 2008: Validation of the Aura MLS cloud Ice Water Content (IWC) measurements. *J. Geophys. Res.,* **113,** doi:10.1029/2007JD008931.

Zhang, Z., S. Platnick, P. Yang, A. K. Heidinger, and J. Comstock, 2010: Effects of ice particle size vertical inhomogeneity on the passive remote sensing of ice clouds. *J. Geophys. Res.,* **115,** D17203, doi:10.1029/2010JD013835.